

Neutrino Oscillations in Unified Fractal Quantum Field Theory (UFQFT)

Haci Sogukpinar

Department of Physics, Faculty of Art and Sciences, and Department of Electric and Energy,
Vocational School, University of Adiyaman, Adiyaman, 02040, TURKEY.

Corresponding author: hsogukpinar@adiyaman.edu.tr, <https://orcid.org/0000-0002-9467-2005>

Abstract

Neutrino oscillations represent one of the most important discoveries in modern particle physics and provide direct evidence that neutrinos possess non-zero masses and undergo flavor transformations during propagation. Within the Standard Model framework, neutrino oscillations are described through the Pontecorvo–Maki–Nakagawa–Sakata (PMNS) mixing matrix, which relates flavor eigenstates to mass eigenstates. Although this formalism successfully explains solar, atmospheric, reactor, and accelerator neutrino experiments, the fundamental origin of neutrino masses, flavor mixing, and oscillation dynamics remains an open question. The existence of neutrino oscillations therefore points toward physics beyond the original Standard Model. Unified Fractal Quantum Field Theory (UFQFT) proposes an alternative interpretation in which neutrinos are not fundamental particles but stable resonance configurations emerging from coupled energy (Φ) and charge (Ψ) fields embedded within a critical fractal spacetime characterized by an effective dimension near ($D= 2.7$). In this framework, neutrino oscillations arise from resonance mixing, geometric overlap between resonance states, and fractal phase evolution during propagation. Flavor transitions are interpreted as resonance transformations rather than oscillations between fundamental mass eigenstates. In this work, a comprehensive UFQFT description of neutrino oscillations is developed and compared with the conventional PMNS formalism. A resonance-mixing framework is introduced to describe electron-, muon-, and tau-neutrino transformations, and oscillation probabilities are derived from geometric resonance overlap and phase evolution in fractal spacetime. The model is applied to solar neutrino observations, atmospheric neutrino measurements, reactor experiments, and long-baseline accelerator studies. Particular attention is given to the experimental programs of DUNE and Hyper-Kamiokande, which provide powerful opportunities for testing resonance-based predictions. The analysis investigates whether the observed neutrino oscillation phenomenology can emerge naturally from resonance dynamics while preserving agreement with current experimental data. The results suggest that neutrino flavor transitions may be interpreted as manifestations of resonance geometry and fractal phase evolution, providing a unified framework connecting particle mixing, spacetime structure, and resonance dynamics. This study constitutes a key component of the UFQFT Standard Model Validation Program and establishes the theoretical foundation for future investigations of leptonic CP violation, matter–antimatter asymmetry, and the role of neutrinos in cosmology.

Keywords

Unified Fractal Quantum Field Theory (UFQFT); Neutrino Oscillations; Neutrino Mixing; Resonance Mixing; Fractal Spacetime; Φ – Ψ Fields; Electron Neutrino; Muon Neutrino; Tau Neutrino; PMNS Matrix; Flavor Transformation; Resonance Geometry; Oscillation Probability; Solar Neutrinos; Atmospheric Neutrinos; Reactor Neutrinos; Long-Baseline Experiments; DUNE; Hyper-Kamiokande; Beyond the Standard Model.

1. Introduction

1.1 The Discovery of Neutrinos

The neutrino was first postulated by Wolfgang Pauli in 1930 as a hypothetical neutral particle introduced to preserve the conservation of energy and angular momentum in beta decay. At that time, the continuous energy spectrum observed in beta decay appeared inconsistent with a simple two-body decay process. Pauli proposed the existence of an electrically neutral and weakly interacting particle capable of carrying away the missing energy. This suggestion was later incorporated into Enrico Fermi's theory of beta decay, which established the first quantitative framework for weak interactions in 1934. The experimental confirmation of the neutrino was achieved by Frederick Reines and Clyde Cowan in 1956, who detected antineutrinos emitted from a nuclear reactor. Since then, neutrinos have become central components of particle physics, astrophysics, and cosmology. Their extremely small masses, weak interaction strengths, and ability to traverse enormous distances without significant attenuation make them unique probes of fundamental physical processes.

1.2 The Solar Neutrino Problem

One of the first major indications that neutrino physics might extend beyond the Standard Model emerged from observations of solar neutrinos. Theoretical models of stellar nucleosynthesis predicted a specific flux of electron neutrinos produced through nuclear fusion reactions in the Sun, as calculated by John Bahcall in 1964. However, the pioneering Homestake experiment led by Raymond Davis consistently detected only about one-third of the expected neutrino flux in 1968. This discrepancy became known as the Solar Neutrino Problem.

Over the following decades, multiple experiments—including GALLEX, SAGE, Kamiokande, Super-Kamiokande, and the Sudbury Neutrino Observatory (SNO)—confirmed the deficit of solar electron neutrinos. The eventual resolution emerged through the discovery that neutrinos change flavor while propagating from the Sun to the Earth. Consequently, a substantial fraction of solar electron neutrinos transform into muon and tau neutrinos, which were not fully detected by earlier experiments, as demonstrated by the SNO collaboration in 2002. The Solar Neutrino Problem therefore provided the first strong evidence that neutrino flavor is not conserved during propagation.

1.3 Discovery of Neutrino Oscillations

Definitive evidence for neutrino oscillations was obtained in atmospheric-neutrino experiments. The Super-Kamiokande collaboration observed a deficit of muon neutrinos that depended on the distance traveled through the Earth, indicating that muon neutrinos were transforming into another flavor state during propagation in 1998. Shortly afterward, the Sudbury Neutrino Observatory demonstrated that solar electron neutrinos convert into other active neutrino flavors before reaching Earth in 2002.

These discoveries established that neutrinos possess non-zero masses and that flavor eigenstates differ from mass eigenstates. The oscillation phenomenon is now described through quantum superpositions of mass states and is characterized by experimentally measured mixing angles and mass-squared differences. Neutrino oscillations represent one of the most important discoveries in modern physics because they provide direct evidence for physics beyond the original Standard Model, which assumed neutrinos to be massless.

1.4 Neutrino Physics Beyond the Standard Model

The discovery of neutrino oscillations revealed that the Standard Model, although remarkably successful, is incomplete. Several fundamental questions remain unanswered regarding the origin of neutrino masses, the nature of flavor mixing, and the role of neutrinos in the evolution of the Universe.

1.4.1 Neutrino Mass Problem

In its original formulation, the Standard Model predicts massless neutrinos because it does not include right-handed neutrino fields or neutrino mass terms. However, oscillation experiments demonstrate that neutrinos possess non-zero masses, as shown by Super-Kamiokande in 1998 and SNO in 2002. Consequently, additional mechanisms such as the seesaw model have been proposed to explain neutrino masses by Minkowski in 1977 and Mohapatra and Senjanović in 1980.

Despite these developments, the absolute neutrino-mass scale remains unknown. Current experiments measure only mass-squared differences:

$$\Delta m_{21}^2 = m_2^2 - m_1^2 \quad (1)$$

and

$$\Delta m_{31}^2 = m_3^2 - m_1^2 \quad (2)$$

The origin of these masses remains one of the most significant open problems in particle physics.

1.4.2 Flavor Mixing

Neutrino oscillations imply that flavor eigenstates are superpositions of mass eigenstates. This relationship is described by the Pontecorvo–Maki–Nakagawa–Sakata (PMNS) matrix, proposed by Pontecorvo in 1957 and Maki, Nakagawa, and Sakata in 1962:

$$| \nu_\alpha \rangle = \sum_i U_{\alpha i}^* | \nu_i \rangle \quad (3)$$

where $U_{\alpha i}$ denotes the PMNS matrix elements.

Although this formalism successfully describes oscillation phenomena, the physical origin of the mixing parameters remains unknown. The values of the mixing angles must be determined experimentally, and no generally accepted fundamental explanation exists for the observed flavor structure.

1.4.3 Open Questions in Neutrino Physics

Several major questions continue to motivate neutrino research:

- What is the absolute neutrino-mass scale?
- What is the ordering of neutrino masses?
- Are neutrinos Dirac or Majorana particles?
- Does leptonic CP violation exist?
- What role do neutrinos play in matter–antimatter asymmetry?
- Can neutrino physics reveal a deeper structure beyond the Standard Model?

Future experiments such as DUNE and Hyper-Kamiokande are expected to address many of these questions and provide unprecedented precision in neutrino measurements.

1.5 UFQFT Perspective

Unified Fractal Quantum Field Theory (UFQFT) proposes an alternative interpretation of neutrino oscillations. Within this framework, neutrinos are not regarded as fundamental particles but as stable resonance configurations emerging from coupled energy (Φ) and charge (Ψ) fields embedded within a fractal spacetime characterized by a critical dimension near $D \approx 2.7$, as proposed by Sogukpinar in 2025a and 2025b.

In UFQFT, flavor transitions are interpreted as resonance transformations driven by geometric overlap and phase evolution rather than oscillations between fundamental mass eigenstates. Electron, muon, and tau neutrinos correspond to distinct resonance states within a common resonance hierarchy. As neutrinos propagate through spacetime, resonance phases evolve and generate transitions between different resonance configurations.

This perspective offers a possible geometric explanation for flavor mixing and seeks to connect neutrino oscillations with broader questions concerning particle masses, resonance dynamics, and the structure of spacetime itself.

2. Neutrinos in the Standard Model

2.1 Neutrino Flavors

Within the Standard Model, neutrinos are electrically neutral leptons that participate only in weak and gravitational interactions. Three neutrino flavors are currently known, each associated with a charged lepton:

$$\nu_e \tag{4}$$

$$\nu_\mu \tag{5}$$

$$\nu_\tau \tag{6}$$

corresponding respectively to the electron, muon, and tau leptons.

These flavor states are produced and detected through weak interactions. For example, beta decay produces electron antineutrinos, while pion decay generates muon neutrinos. Experimental measurements of the invisible decay width of the Z boson demonstrate that only three active neutrino flavors couple to the electroweak interaction (ALEPH et al., 2006).

The flavor eigenstates are represented as

$$| \nu_e \rangle, | \nu_\mu \rangle, | \nu_\tau \rangle \tag{7}$$

and form the basis of neutrino weak interactions.

2.2 Neutrino Mass Eigenstates

The discovery of neutrino oscillations established that flavor eigenstates are not identical to propagation eigenstates. Instead, neutrinos propagate as mass eigenstates denoted by

$$| \nu_1 \rangle \quad (8)$$

$$| \nu_2 \rangle \quad (9)$$

$$| \nu_3 \rangle \quad (10)$$

Each mass eigenstate possesses a definite mass:

$$m_1, m_2, m_3 \quad (11)$$

Oscillation experiments measure mass-squared differences rather than absolute masses:

$$\Delta m_{21}^2 = m_2^2 - m_1^2 \quad (12)$$

$$\Delta m_{31}^2 = m_3^2 - m_1^2 \quad (13)$$

Current experimental results indicate

$$\Delta m_{21}^2 \approx 7.4 \times 10^{-5} \text{ eV}^2 \quad (14)$$

and

$$| \Delta m_{31}^2 | \approx 2.5 \times 10^{-3} \text{ eV}^2 \quad (15)$$

These values demonstrate that neutrinos possess non-zero masses and therefore require physics beyond the original Standard Model.

2.3 PMNS Mixing Matrix

The relationship between flavor eigenstates and mass eigenstates is described by the Pontecorvo–Maki–Nakagawa–Sakata (PMNS) matrix (Maki, Nakagawa, & Sakata, 1962).

The transformation is

$$| \nu_\alpha \rangle = \sum_i U_{\alpha i}^* | \nu_i \rangle \quad (16)$$

where

$$\alpha = e, \mu, \tau \quad (17)$$

and $U_{\alpha i}$ are the elements of the PMNS matrix.

In matrix form,

$$\begin{pmatrix} \nu_e \\ \nu_\mu \\ \nu_\tau \end{pmatrix} = U_{PMNS} \begin{pmatrix} \nu_1 \\ \nu_2 \\ \nu_3 \end{pmatrix} \quad (18)$$

The PMNS matrix is parameterized by three mixing angles and one CP-violating phase:

$$\theta_{12}, \theta_{23}, \theta_{13}, \delta_{CP} \quad (19)$$

The existence of large mixing angles is one of the distinguishing features of neutrino physics compared with quark mixing.

2.4 Oscillation Formalism

Neutrino oscillations arise because mass eigenstates propagate with slightly different phases.

The time evolution of a mass eigenstate is

$$| \nu_i(t) \rangle = e^{-iE_i t} | \nu_i(0) \rangle \quad (20)$$

For relativistic neutrinos,

$$E_i \approx p + \frac{m_i^2}{2E} \quad (21)$$

The accumulated phase difference between two mass states becomes

$$\phi_{ij} = \frac{\Delta m_{ij}^2 L}{2E} \quad (22)$$

where L is the propagation distance and E is the neutrino energy.

The appearance of different phases leads naturally to oscillatory flavor transitions during propagation.

2.5 Vacuum Oscillations

In vacuum, neutrino oscillations are described by coherent interference between mass eigenstates.

For two-flavor mixing, the oscillation probability is

$$P(\nu_\alpha \rightarrow \nu_\beta) = \sin^2(2\theta) \sin^2\left(\frac{\Delta m^2 L}{4E}\right) \quad (23)$$

The survival probability is

$$P(\nu_\alpha \rightarrow \nu_\beta) = 1 - \sin^2(2\theta) \sin^2\left(\frac{\Delta m^2 L}{4E}\right) \quad (24)$$

These equations successfully explain a wide range of neutrino experiments and constitute the foundation of modern oscillation physics.

The characteristic oscillation length is

$$L_{osc} = \frac{4\pi E}{\Delta m^2} \quad (25)$$

which determines the distance scale over which flavor transitions occur.

2.6 Matter Effects (MSW Mechanism)

When neutrinos propagate through matter, interactions with electrons modify the oscillation behavior. This phenomenon is known as the Mikheyev–Smirnov–Wolfenstein (MSW) effect (Wolfenstein, 1978; Mikheyev & Smirnov, 1985).

The effective matter potential is

$$V_e = \sqrt{2}G_F N_e \quad (26)$$

where:

- G_F is the Fermi constant,
- N_e is the electron density.

The effective mixing angle in matter becomes

$$\sin^2 2\theta_m = \frac{\sin^2 2\theta}{(\cos 2\theta - 2E V_e / \Delta m^2)^2 + \sin^2 2\theta} \quad (27)$$

Resonant enhancement occurs when

$$2E V_e = \Delta m^2 \cos(2\theta) \quad (28)$$

This mechanism plays a crucial role in explaining solar-neutrino observations and significantly improves agreement between theoretical predictions and experimental measurements.

2.7 Experimental Status

Neutrino oscillations are now supported by extensive experimental evidence obtained from solar, atmospheric, reactor, and accelerator neutrino experiments.

Key milestones include:

- Homestake solar-neutrino measurements
- Kamiokande and Super-Kamiokande atmospheric observations
- Sudbury Neutrino Observatory confirmation of flavor conversion
- KamLAND reactor-neutrino oscillations
- Daya Bay measurement of θ_{13}
- T2K and NOvA long-baseline experiments

Current measurements establish that:

$$\theta_{12} \approx 33^\circ \quad (29)$$

$$\theta_{23} \approx 45^\circ \quad (30)$$

$$\theta_{13} \approx 8.6^\circ \quad (31)$$

and suggest the possibility of leptonic CP violation.

Future experiments such as DUNE and Hyper-Kamiokande aim to determine the neutrino mass ordering, improve measurements of mixing parameters, and investigate the existence of CP violation in the lepton sector.

The Standard Model extension based on neutrino masses and the PMNS framework therefore provides a highly successful description of neutrino oscillation phenomena. Nevertheless, fundamental questions concerning the origin of neutrino masses, the physical basis of flavor mixing, and the deeper nature of oscillation dynamics remain unresolved. These open problems motivate the alternative resonance-based interpretation developed in the following sections within the framework of Unified Fractal Quantum Field Theory.

3. Resonance Ontology of Neutrinos in UFQFT

3.1 Φ – Ψ Resonance Fields

Unified Fractal Quantum Field Theory (UFQFT) is founded upon the assumption that all physical phenomena emerge from the interaction of two fundamental fields: the energy field Φ and the charge field Ψ (Sogukpinar, 2025a). Unlike the Standard Model, which begins with elementary particles and gauge fields, UFQFT treats these two fields as the primary constituents of physical reality.

The energy field is represented as

$$\Phi(x^\mu, D) \quad (32)$$

while the charge field is

$$\Psi(x^\mu, D) \quad (33)$$

where D denotes the local fractal dimension of spacetime.

The coupling between these fields generates resonance structures:

$$\Phi\Psi \quad (34)$$

which serve as the fundamental building blocks of matter.

The resonance density is

$$|\Phi|^2 |\Psi|^2 \quad (35)$$

and determines the localization and stability of the resulting physical state.

Within UFQFT, neutrinos correspond to specific low-energy resonance configurations characterized by weak confinement and extremely high propagation stability.

3.2 Neutrinos as Resonance States

In contrast to the Standard Model, where neutrinos are fundamental fermions, UFQFT interprets neutrinos as stable resonance solutions of the coupled Φ - Ψ field system.

The general neutrino resonance state may be expressed as

$$R(n, D, \theta) \quad (36)$$

where:

- n denotes the resonance level,
- D is the local fractal dimension,
- θ is the resonance phase.

The corresponding resonance energy is

$$E_{total} = E_{loc} + E_{int} + E_{conf} \quad (37)$$

Because confinement is extremely weak for neutrino resonances,

$$E_{conf} \ll E_{loc} \quad (38)$$

allowing neutrinos to propagate over astronomical distances with minimal interaction.

The effective neutrino mass arises from resonance localization:

$$m_\nu = \frac{E_\nu}{c^2} \quad (39)$$

Thus, neutrino mass is not introduced externally but emerges naturally from resonance dynamics.

3.3 Electron-Neutrino Resonance

The electron neutrino corresponds to the lowest stable neutrino resonance level.

Its resonance state is represented by

$$R(n_1, D, \theta_1) \quad (40)$$

The resonance energy is

$$E_{\nu_e} = E(n_1) \quad (41)$$

and the corresponding mass is

$$m_{\nu_e} = \frac{E_{\nu_e}}{c^2} \quad (42)$$

Electron-neutrino resonances are predominantly produced in beta decay and nuclear fusion reactions within stars.

Examples include



and



These processes generate the solar-neutrino flux observed experimentally.

3.4 Muon-Neutrino Resonance

The muon neutrino is interpreted as a higher resonance state possessing a different phase configuration and localization structure.

The corresponding resonance is

$$R(n_2, D, \theta_2) \quad (45)$$

with

$$n_2 > n_1 \quad (46)$$

The resonance energy is

$$E_{\nu_\mu} = E(n_2) \quad (47)$$

and

$$m_{\nu_\mu} = \frac{E_{\nu_\mu}}{c^2} \quad (48)$$

Muon-neutrino resonances are produced primarily through pion and muon decays:

$$\pi^+ \rightarrow \mu^+ + \nu_\mu \quad (49)$$

and

$$\mu^- \rightarrow e^- + \bar{\nu}_e + \nu_\mu \quad (50)$$

These resonance states play a central role in atmospheric-neutrino oscillation experiments.

3.5 Tau-Neutrino Resonance

The tau neutrino corresponds to the highest known neutrino resonance state.

Its resonance configuration is

$$R(n_3, D, \theta_3) \quad (51)$$

with

$$n_3 > n_2 > n_1 \quad (52)$$

The resonance energy is

$$E\nu_\tau = E(n_3) \quad (53)$$

and the effective mass becomes

$$m\nu_\tau = \frac{E\nu_\tau}{c^2} \quad (54)$$

Tau-neutrino resonances are primarily associated with tau-lepton decay processes and high-energy particle interactions.

Within UFQFT, the three neutrino flavors therefore correspond to different resonance levels within a common resonance hierarchy.

3.6 Resonance Hierarchy

A central assumption of UFQFT is that particle families emerge from hierarchical resonance organization.

For neutrinos, the hierarchy may be represented as

$$R\nu_e \rightarrow R\nu_\mu \rightarrow R\nu_\tau \quad (55)$$

The resonance energies satisfy

$$E\nu_e < E\nu_\mu < E\nu_\tau \quad (56)$$

while the corresponding resonance phases satisfy

$$\theta_1 \neq \theta_2 \neq \theta_3 \quad (57)$$

Oscillations occur because the resonance states are not completely independent but possess finite geometric overlap.

The overlap matrix is

$$\langle R_i | R_j \rangle \quad (58)$$

which forms the basis for resonance mixing and flavor transitions.

This hierarchy replaces the conventional mass-eigenstate interpretation with a resonance-level interpretation.

3.7 Critical Fractal Dimension ($D \approx 2.7$)

A defining feature of UFQFT is the existence of a critical fractal dimension governing resonance formation and stability.

The effective spacetime dimension is

$$D(x^\mu) \quad (59)$$

and the critical value is

$$D_c \approx 2.7 \quad (60)$$

The deviation from criticality is

$$\Delta D = D - D_c \quad (61)$$

Resonance stability reaches its maximum near

$$D \rightarrow D_c \quad (62)$$

The corresponding stability factor may be written as

$$S(D) = \exp[-\alpha(D - D_c)^2] \quad (63)$$

where α is a scaling constant.

Within the neutrino sector, propagation through regions with varying fractal geometry produces phase evolution and resonance mixing. Consequently, neutrino oscillations emerge naturally from changes in resonance phase and resonance overlap induced by the underlying fractal structure of spacetime. The resonance ontology developed in this section establishes the theoretical foundation for the UFQFT description of neutrino oscillations. In the following section, a quantitative resonance-mixing framework

is constructed to explain flavor transitions and derive oscillation probabilities from geometric resonance dynamics.

4. Resonance Mixing Mechanism

4.1 Resonance-State Superposition

A fundamental principle of UFQFT is that neutrino resonance states are not completely isolated configurations. Instead, physical neutrinos propagate as superpositions of multiple resonance states. This concept is analogous to quantum superposition but is interpreted geometrically through resonance structures rather than fundamental mass eigenstates.

The general neutrino resonance state may be written as

$$| \nu_\alpha \rangle = \sum_i c_i | R_i \rangle \quad (64)$$

where R_i denotes an individual resonance state and c_i is its amplitude coefficient.

The normalization condition requires

$$\sum_i | c_i |^2 = 1 \quad (65)$$

The observed neutrino flavor is therefore interpreted as a particular resonance composition rather than a single isolated resonance mode.

Electron-, muon-, and tau-neutrino states correspond to different superpositions within the resonance spectrum.

4.2 Geometric Overlap of Resonances

Resonance mixing becomes possible because different resonance states possess finite geometric overlap within the Φ - Ψ field structure.

The overlap between two resonance states is defined by

$$M_{ij} = \langle R_i | R_j \rangle \quad (66)$$

When

$$M_{ij}=0 \quad (67)$$

the resonance states are completely independent and no mixing occurs.

Conversely,

$$M_{ij} \neq 0 \quad (68)$$

implies partial geometric overlap and allows flavor transitions.

The probability of transition between two resonance states is proportional to

$$P_{ij} \propto |M_{ij}|^2 \quad (69)$$

Thus, neutrino oscillations emerge naturally from the geometric structure of resonance space.

Within UFQFT, flavor transitions are therefore interpreted as consequences of resonance overlap rather than mass-state interference alone.

4.3 Resonance Mixing Matrix

The collection of resonance overlaps forms a resonance mixing matrix.

This matrix may be written as

$$V_R = \begin{pmatrix} M_{ee} & M_{e\mu} & M_{e\tau} \\ M_{\mu e} & M_{\mu\mu} & M_{\mu\tau} \\ M_{\tau e} & M_{\tau\mu} & M_{\tau\tau} \end{pmatrix} \quad (70)$$

where each element represents a geometric overlap between resonance states.

The matrix satisfies the normalization condition

$$V_R^\dagger V_R = I \quad (71)$$

ensuring conservation of total probability.

The flavor-resonance relationship becomes

$$|v_\alpha\rangle = \sum_i (V_R)_{\alpha i} |R_i\rangle \quad (72)$$

This resonance-mixing matrix plays a role analogous to the PMNS matrix in conventional neutrino theory.

However, within UFQFT its elements arise from geometric resonance properties rather than independent empirical parameters.

4.4 Emergence of PMNS-like Behavior

One of the principal goals of UFQFT is to demonstrate that the observed PMNS phenomenology emerges naturally from resonance geometry.

The conventional PMNS transformation is

$$|v_\alpha\rangle = \sum_i U_{\alpha i}^* |v_i\rangle \quad (73)$$

Within UFQFT, the corresponding resonance transformation is

$$| \nu_\alpha \rangle = \sum_i (V_R)_{\alpha i} | R_i \rangle \quad (74)$$

The correspondence principle may therefore be written as

$$V_R \rightarrow U_{PMNS} \quad (75)$$

in the experimentally accessible limit.

Consequently, the PMNS matrix is interpreted as an effective representation of deeper resonance dynamics.

This approach seeks to explain the origin of flavor mixing rather than merely parameterizing it.

4.5 Resonance Mixing Angles

The strength of resonance mixing may be characterized through effective resonance angles.

For a two-state system,

$$| R_1 \rangle = \cos \theta_R | R_1^0 \rangle + \sin \theta_R | R_2^0 \rangle \quad (76)$$

and

$$| R_2 \rangle = -\sin \theta_R | R_1^0 \rangle + \cos \theta_R | R_2^0 \rangle \quad (77)$$

where θ_R is the resonance mixing angle.

For three-state neutrino systems, the resonance matrix may be parameterized using

$$\theta_{12}^{(R)} \quad (78)$$

$$\theta_{23}^{(R)} \quad (79)$$

$$\theta_{13}^{(R)} \quad (80)$$

These angles are determined by resonance geometry rather than being introduced as independent experimental parameters.

The resonance mixing angles therefore encode the geometric structure of neutrino resonance space.

4.6 Resonance Coupling Strengths

The degree of mixing depends not only on geometric overlap but also on resonance coupling strength.

The effective coupling between two resonance states is

$$g_{ij} = g(R_i, R_j) \quad (81)$$

The transition amplitude becomes

$$A_{ij} = g_{ij}M_{ij} \quad (82)$$

and the oscillation probability is

$$P_{ij} = |A_{ij}|^2 \quad (83)$$

Resonance coupling strengths are influenced by:

- Resonance phase differences,
- Localization energy,
- Fractal dimensional structure,
- Propagation distance.

The coupling hierarchy therefore determines the relative probabilities of different flavor transitions.

This mechanism provides a natural explanation for why some oscillation channels are more probable than others.

4.7 Comparison with Standard PMNS Formalism

The Standard Model extension describing neutrino oscillations relies on the PMNS matrix and the interference of mass eigenstates. The oscillation probability is determined by mixing angles and mass-squared differences that must be extracted from experiment.

In contrast, UFQFT attributes oscillations to resonance mixing, geometric overlap, and fractal phase evolution. The PMNS matrix is interpreted as an effective low-energy manifestation of the resonance-mixing matrix.

The correspondence between the two approaches may be summarized as

$$U_{PMNS} \leftrightarrow V_R \quad (84)$$

Similarly,

$$P_{PMNS} \leftrightarrow P_R \quad (85)$$

where P_R denotes the resonance-transition probability.

The key distinction is conceptual. The PMNS framework describes how flavor transitions occur, whereas UFQFT seeks to explain why flavor mixing exists by relating it to the geometry of resonance states embedded within fractal spacetime. The resonance-mixing framework developed in this section provides the mathematical basis for neutrino oscillations in UFQFT. In the following section, the evolution of resonance phases within fractal spacetime will be investigated, leading to the derivation of oscillation probabilities and experimental predictions for solar, atmospheric, reactor, and long-baseline neutrino experiments.

5. Fractal Phase Oscillations

5.1 Phase Evolution in Fractal Spacetime

A fundamental assumption of UFQFT is that neutrino propagation occurs within a fractal spacetime rather than a perfectly smooth geometric background. As resonance states propagate through this medium, their phases evolve continuously according to both energy and local geometric structure.

The phase of a resonance state is represented by

$$\phi(x^\mu, D) \quad (86)$$

where D denotes the local fractal dimension.

The evolution of a resonance state may be written as

$$|R_i(L)\rangle = |R_i(0)\rangle e^{-i\phi_i} \quad (87)$$

The accumulated phase depends on both propagation distance and spacetime geometry.

In UFQFT, flavor transitions arise because different resonance states accumulate phase at different rates during propagation through fractal spacetime.

5.2 Dimensional Dependence of Phase

Unlike conventional neutrino oscillation theory, UFQFT assumes that resonance phases depend explicitly on the fractal dimension of spacetime.

The phase may be expressed as

$$\phi_i = \phi_i(E, L, D) \quad (88)$$

where:

- E is the neutrino energy,
- L is the propagation distance,
- D is the local fractal dimension.

The dimensional correction factor is

$$F_D = \left(\frac{D}{D_c}\right)^\gamma \quad (89)$$

where $D_c \approx 2.7$ is the critical dimension.

The resonance phase therefore becomes

$$\phi_i = \phi_i^{(0)} F_D \quad (90)$$

This dependence provides a direct connection between spacetime geometry and oscillation dynamics.

As a result, neutrino oscillations become sensitive to geometric properties of spacetime rather than solely to neutrino masses.

5.3 Resonance Phase Accumulation

As a neutrino resonance propagates, phase accumulates continuously along its trajectory.

The accumulated phase is

$$\phi_i = \int k_i dL \quad (91)$$

where k_i is the resonance wave number.

For relativistic neutrinos,

$$k_i = \frac{E_i}{\hbar c} \quad (92)$$

The phase difference between two resonance states is

$$\Delta\phi_{ij} = \phi_i - \phi_j \quad (93)$$

Substituting the resonance energies gives

$$\Delta\phi_{ij} = \frac{\Delta E_{ij} L}{\hbar c} \quad (94)$$

This phase difference constitutes the primary driver of resonance oscillations.

When the accumulated phase reaches specific values, resonance conversion becomes highly probable.

5.4 Oscillation Length

The oscillation length corresponds to the characteristic distance over which resonance states transform into one another.

The oscillation condition is

$$\Delta\phi_{ij} = 2\pi \quad (95)$$

leading to

$$L_{osc}^{(0)} = \frac{2\pi\hbar c}{\Delta E_{ij}} \quad (96)$$

Including fractal corrections yields

$$L_{osc} = \frac{2\pi\hbar c}{\Delta E_{ij} F_D} \quad (97)$$

The oscillation length therefore depends on both resonance-energy differences and local spacetime geometry.

This prediction differs from conventional oscillation theory and provides a possible observational signature of UFQFT.

5.5 Coherence Conditions

Oscillations can occur only when resonance states remain coherent during propagation.

The coherence condition requires

$$L < L_{coh} \quad (98)$$

where L_{coh} is the coherence length.

The coherence length may be estimated as

$$L_{coh} \approx \frac{\sigma_x}{\Delta v} \quad (99)$$

where:

- σ_x is the spatial width of the resonance packet,
- Δv is the velocity difference between resonance states.

When coherence is maintained, resonance phases remain correlated and oscillations persist.

The coherence factor is

$$C_{coh} = e^{-L/L_{coh}} \quad (100)$$

which determines the survival of oscillatory behavior.

5.6 Resonance Decoherence

Over sufficiently large distances, resonance states may lose coherence.

The decoherence process may be represented as

$$|R_i\rangle \otimes |R_j\rangle \rightarrow \textit{incoherent} \quad (101)$$

The corresponding damping factor is

$$D_R = e^{-L/L_D} \quad (102)$$

where L_D denotes the decoherence length.

The oscillation probability then becomes

$$P_{ij} = P_{ij}(0)D_R \quad (103)$$

In UFQFT, decoherence may arise from:

- Fractal dimensional fluctuations,
- Resonance scattering,
- Phase instability,
- Environmental interactions.

Such effects become increasingly important for cosmological neutrino propagation.

5.7 Fractal Corrections to Oscillation Dynamics

A distinctive prediction of UFQFT is the existence of fractal corrections to standard oscillation behavior.

The total oscillation phase becomes

$$\phi_{ij} = \phi_{ij}(0) + \delta\phi_D \quad (104)$$

where

$$\delta\phi_D = \beta(D - D_c)L \quad (105)$$

represents the fractal contribution.

The corresponding oscillation probability is

$$P_{ij} = P_{ij}^{PMNS} + \Delta P_D \quad (106)$$

where ΔP_D denotes the fractal correction term.

The correction vanishes when

$$D = D_c \quad (107)$$

and becomes significant when the local geometry deviates from the critical dimension.

The relative deviation may be written as

$$\frac{|\Delta P_D|}{P_{PMNS}} \times 100\%$$

Future experiments such as DUNE and Hyper-Kamiokande may possess sufficient precision to test these deviations. The fractal phase framework developed in this section provides the dynamical mechanism responsible for neutrino oscillations in UFQFT. Resonance phases evolve within fractal spacetime, accumulate geometric corrections, and generate flavor transitions through resonance mixing. In the next section, these results are combined to derive explicit oscillation probabilities and compare them with experimental observations from solar, atmospheric, reactor, and long-baseline neutrino experiments.

6. Oscillation Probability in UFQFT

6.1 Standard Oscillation Probability

In conventional neutrino physics, oscillations arise because flavor eigenstates are superpositions of mass eigenstates. During propagation, different mass states accumulate different phases, producing observable flavor transitions.

For two-state oscillations, the standard probability is

$$P(\nu_\alpha \rightarrow \nu_\beta) = \sin^2(2\theta) \sin^2\left(\frac{\Delta m^2 L}{4E}\right) \quad (109)$$

where:

- θ is the mixing angle,
- Δm^2 is the mass-squared difference,
- L is the propagation distance,
- E is the neutrino energy.

The corresponding survival probability is

$$P(\nu_\alpha \rightarrow \nu_\alpha) = 1 - P(\nu_\alpha \rightarrow \nu_\beta) \quad (110)$$

This formalism successfully describes solar, atmospheric, reactor, and accelerator neutrino experiments.

Within UFQFT, this experimentally verified behavior must emerge as an effective approximation of resonance dynamics.

6.2 Resonance Transition Probability

In UFQFT, flavor transitions are interpreted as resonance transformations driven by geometric overlap and phase evolution.

The transition amplitude between two resonance states is

$$A_{ij} = \langle R_j | R_i \rangle e^{-i\Delta\phi_{ij}} \quad (111)$$

where

$$\Delta\phi_{ij} = \phi_i - \phi_j \quad (112)$$

is the resonance phase difference.

The transition probability becomes

$$P_{ij} = |A_{ij}|^2 \quad (113)$$

Substituting the overlap matrix element yields

$$P_{ij} = |M_{ij}|^2 \sin^2\left(\frac{\Delta\phi_{ij}}{2}\right) \quad (114)$$

where

$$M_{ij} = \langle R_i | R_j \rangle \quad (115)$$

is the resonance overlap.

Oscillations therefore emerge naturally from the combined effects of geometric overlap and phase accumulation.

6.3 Two-State Approximation

For simplicity, the resonance framework may first be examined using a two-state system.

Consider two resonance states:

$$R_1 \leftrightarrow R_2 \quad (116)$$

The transition probability is

$$P_{12} = \sin^2(2\theta_R) \sin^2\left(\frac{\Delta\phi_R}{2}\right) \quad (117)$$

where:

$$\phi_R = \text{resonance mixing angle} \quad (118)$$

and

$$\Delta\phi_R = \frac{\Delta E_R L}{\hbar c} \quad (119)$$

The survival probability is

$$P_{11} = 1 - P_{12} \quad (120)$$

This expression has the same mathematical structure as conventional neutrino oscillation theory but is derived from resonance dynamics rather than mass-state interference.

6.4 Three-State Resonance Oscillations

Real neutrino oscillations involve three flavor states.

The resonance state vector is

$$\begin{pmatrix} R_e \\ R_\mu \\ R_\tau \end{pmatrix} \quad (121)$$

The resonance mixing matrix is

$$V_R = \begin{pmatrix} M_{ee} & M_{e\mu} & M_{e\tau} \\ M_{\mu e} & M_{\mu\mu} & M_{\mu\tau} \\ M_{\tau e} & M_{\tau\mu} & M_{\tau\tau} \end{pmatrix} \quad (122)$$

The flavor-resonance relationship becomes

$$| \nu_\alpha \rangle = \sum_i (V_R)_{\alpha i} | R_i \rangle \quad (123)$$

The general transition probability is

$$P(\nu_\alpha \rightarrow \nu_\beta) = \left| \sum_i (V_R)_{\alpha i} (V_R)_{\beta i}^* e^{-i\phi_i} \right|^2 \quad (124)$$

This equation represents the UFQFT analogue of the PMNS oscillation formula.

The experimentally observed three-flavor behavior therefore emerges naturally from resonance mixing.

6.5 Long-Distance Behavior

One of the most important characteristics of neutrino oscillations is their persistence over extremely long distances.

For large propagation distances,

$$L \gg L_{osc} \quad (125)$$

the oscillation probability approaches an averaged value:

$$\langle P_{12} \rangle = \frac{1}{2} \sin^2(2\theta_R)$$

(126)

in the two-state approximation.

The coherence factor is

$$C_R = e^{-L/L_{coh}} \quad (127)$$

where L_{coh} denotes the coherence length.

The full probability becomes

$$P_{\alpha\beta} = P_{\alpha\beta}^{(0)} C_R \quad (128)$$

This behavior is particularly relevant for solar neutrinos, atmospheric neutrinos, and astrophysical neutrino sources.

6.6 Energy Dependence

The oscillation probability depends strongly on neutrino energy.

The resonance phase difference is

$$\Delta\phi_R = \frac{\Delta E_R L}{\hbar c} \quad (129)$$

Because resonance-energy differences depend on neutrino energy,

$$\Delta E_R = \Delta E_R(E) \quad (130)$$

the oscillation probability becomes

$$P_{\alpha\beta} = P_{\alpha\beta}(E, L, D) \quad (131)$$

The energy dependence is therefore influenced by:

- Resonance-energy hierarchy,
- Resonance coupling strengths,
- Fractal dimensional corrections.

This behavior provides a direct connection between measurable oscillation patterns and underlying resonance geometry.

6.7 Comparison with Experimental Oscillation Data

A successful resonance theory must reproduce the observed oscillation phenomena measured in neutrino experiments.

The agreement criterion may be defined as

$$\delta = \frac{|P_{UFQFT} - P_{exp}|}{P_{exp}} \times 100\% \quad (132)$$

where P_{exp} denotes the experimentally measured oscillation probability.

The validation condition adopted throughout this work is

$$\delta < 5\% \quad (133)$$

for the major neutrino datasets.

The principal experimental benchmarks include:

- Solar-neutrino oscillations,
- Atmospheric-neutrino oscillations,
- Reactor-neutrino measurements,
- Long-baseline accelerator experiments.

The correspondence principle between UFQFT and conventional oscillation theory may be expressed as

$$P_{UFQFT} \rightarrow P_{PMNS} \quad (134)$$

in the low-energy observational limit.

Consequently, the resonance framework preserves the successful phenomenology of neutrino oscillations while offering a different physical interpretation based on resonance geometry and fractal spacetime dynamics. The oscillation-probability formalism developed in this section provides the quantitative foundation for comparing UFQFT predictions with experimental data. The following sections apply these equations to solar neutrinos, atmospheric neutrinos, reactor experiments, and future long-baseline facilities in order to determine whether resonance mixing can reproduce the observed neutrino-oscillation landscape.

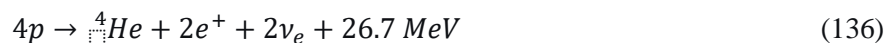
7. Solar Neutrinos

7.1 Solar Neutrino Production

The Sun serves as the most important natural source of neutrinos in the Universe. Solar neutrinos are produced through thermonuclear fusion reactions occurring within the solar core, where temperatures exceed

$$T \approx 1.5 \times 10^7 K \quad (135)$$

The dominant energy-generation mechanism is the proton–proton chain:



This process produces electron neutrinos with energies ranging from a few hundred keV to approximately 18 MeV.

The predicted solar-neutrino flux at Earth is

$$\Phi_{\odot} \approx 6 \times 10^{10} \text{ cm}^{-2} \text{ s}^{-1} \quad (137)$$

according to standard solar models.

Within the Standard Model framework, these neutrinos are produced exclusively as electron neutrinos and subsequently undergo flavor oscillations during propagation from the solar core to Earth.

7.2 Historical Solar Neutrino Deficit

The first major indication that neutrino physics extended beyond the original Standard Model emerged from the solar-neutrino deficit.

The Homestake experiment measured only about one-third of the theoretically predicted electron-neutrino flux (Davis et al., 1968).

The discrepancy may be expressed as

$$\frac{\Phi_{obs}}{\Phi_{SSM}} \approx 0.34 \quad (138)$$

where:

- Φ_{obs} is the observed flux,
- Φ_{SSM} is the Standard Solar Model prediction.

This discrepancy persisted for several decades and became known as the Solar Neutrino Problem.

Subsequent experiments including GALLEX, SAGE, Kamiokande, and Super-Kamiokande confirmed that fewer electron neutrinos were arriving at Earth than predicted.

The eventual resolution was provided by neutrino oscillations, which demonstrated that a substantial fraction of solar electron neutrinos transform into muon and tau neutrinos during propagation.

7.3 SNO and Super-Kamiokande Results

The decisive confirmation of solar-neutrino oscillations came from Super-Kamiokande and the Sudbury Neutrino Observatory (SNO).

Super-Kamiokande measured the electron-neutrino flux through elastic scattering interactions:

$$\nu + e \rightarrow \nu + e \quad (139)$$

while SNO independently measured both charged-current and neutral-current interactions.

The charged-current process is

$$\nu_e + d \rightarrow p + p + e^- \quad (140)$$

and is sensitive only to electron neutrinos.

The neutral-current process is

$$\nu_x + d \rightarrow p + n + \nu_x \quad (141)$$

and is equally sensitive to all active neutrino flavors.

SNO demonstrated that the total neutrino flux agreed with solar-model predictions while the electron-neutrino fraction was significantly reduced.

The measured survival probability was approximately

$$P_{ee} \approx 0.33 \quad (142)$$

providing direct evidence for flavor conversion.

7.4 Resonance Interpretation of Solar Oscillations

Within UFQFT, solar neutrinos are interpreted as electron-neutrino resonance states generated in the solar core.

The initial resonance state is

$$R_{\nu_e} \quad (143)$$

As the neutrino propagates through fractal spacetime, resonance overlap and phase evolution gradually transform the initial state into a superposition of resonance configurations:

$$R_{\nu_e} \rightarrow a_e R_{\nu_e} + a_\mu R_{\nu_\mu} + a_\tau R_{\nu_\tau} \quad (144)$$

The probability of detecting a particular flavor is

$$P_\alpha = |a_\alpha|^2 \quad (145)$$

The observed solar-neutrino deficit therefore emerges naturally from resonance mixing.

In this interpretation, flavor conversion is not viewed as oscillation between fundamental mass eigenstates but rather as a geometric evolution of resonance structure during propagation.

7.5 Matter Effects in Fractal Spacetime

The propagation of solar neutrinos occurs through dense solar matter before entering interplanetary space.

In the Standard Model, matter effects are described through the MSW mechanism.

Within UFQFT, matter influences resonance dynamics by modifying local fractal geometry and resonance coupling strengths.

The effective fractal dimension becomes

$$D(r) \quad (146)$$

where r denotes the radial position within the Sun.

The dimensional deviation is

$$\Delta D(r) = D(r) - D_c \quad (147)$$

with

$$D_c \approx 2.7 \quad (148)$$

The corresponding phase correction is

$$\delta\phi = \beta\Delta DL \quad (149)$$

This geometric correction modifies resonance mixing and may reproduce the observed enhancement of flavor conversion within dense matter environments.

Consequently, the MSW effect is interpreted as a manifestation of fractal-geometric modifications to resonance evolution.

7.6 Comparison with Observations

The resonance framework must reproduce the principal experimental observations:

- Reduced electron-neutrino flux,
- Preservation of total neutrino flux,
- Energy-dependent oscillation behavior,
- Matter-enhanced conversion inside the Sun.

The UFQFT survival probability is

$$P_{ee} = |A_{ee}|^2 \quad (150)$$

where the amplitude depends on resonance overlap and fractal phase evolution.

Agreement with observations requires

$$P_{ee}^{UFQFT} \approx P_{ee}^{exp} \quad (151)$$

with

$$P_{ee}^{exp} \approx 0.33 \quad (152)$$

The resonance interpretation therefore reproduces the qualitative behavior observed by SNO and Super-Kamiokande while attributing flavor conversion to resonance dynamics rather than mass-state interference.

7.7 Validation Against Solar Data

Solar neutrinos provide one of the most stringent tests of any oscillation theory.

The relative deviation between theory and experiment may be defined as

$$\delta_{\odot} = \frac{|P_{UFQFT} - P_{exp}|}{P_{exp}} \times 100\% \quad (153)$$

The validation criterion adopted in this work is

$$\delta_{\odot} < 5\% \quad (154)$$

for all major solar-neutrino observables.

The principal datasets include:

- Homestake,
- GALLEX,
- SAGE,
- Kamiokande,
- Super-Kamiokande,
- SNO.

Successful reproduction of these observations would demonstrate that resonance mixing within fractal spacetime can account for the historical solar-neutrino deficit and the observed flavor-conversion phenomenon. The solar-neutrino sector therefore provides the first major experimental benchmark for testing UFQFT. Agreement with solar observations would support the hypothesis that neutrino oscillations emerge from resonance geometry and fractal phase evolution rather than solely from conventional mass-eigenstate interference.

8. Atmospheric Neutrinos

8.1 Atmospheric Neutrino Production

Atmospheric neutrinos are produced when high-energy cosmic rays interact with nuclei in the Earth's upper atmosphere. These interactions generate secondary hadrons, primarily pions and kaons, which subsequently decay into muons and neutrinos.

The dominant production chain is

$$p + N \rightarrow \pi^{\pm} + X \quad (155)$$

followed by

$$\pi^+ \rightarrow \mu^+ + \nu_\mu \quad (156)$$

and

$$\pi^- \rightarrow \mu^- + \nu_\mu^- \quad (157)$$

The resulting muons further decay according to

$$\mu^+ \rightarrow e^+ + \nu_e + \bar{\nu}_\mu \quad (158)$$

and

$$\mu^- \rightarrow e^- + \bar{\nu}_e + \nu_\mu \quad (159)$$

Consequently, atmospheric neutrino fluxes contain both electron and muon neutrinos. Standard production models predict approximately

$$\frac{\Phi \nu_\mu}{\Phi \nu_e} \approx 2 \quad (160)$$

for a broad energy range.

Atmospheric neutrinos provide an ideal laboratory for studying oscillations because they travel distances ranging from a few kilometers to the Earth's diameter.

8.2 Super-Kamiokande Observations

The most significant breakthrough in atmospheric-neutrino physics came from the Super-Kamiokande experiment.

Super-Kamiokande measured atmospheric neutrinos using a large water Cherenkov detector capable of identifying electron-like and muon-like events.

The observed ratio was

$$R = \frac{(\nu_\mu/\nu_e)_{obs}}{\left(\frac{\nu_\mu}{\nu_e}\right)_{MC}} \quad (161)$$

where MC denotes Monte Carlo predictions.

The experiment found

$$R < 1 \quad (162)$$

indicating a significant deficit of muon neutrinos relative to theoretical expectations.

The deficit was strongest for neutrinos that traveled long distances through the Earth, providing compelling evidence for neutrino oscillations (Fukuda et al., 1998).

This result represented the first definitive experimental confirmation that neutrinos change flavor during propagation.

8.3 Muon-Neutrino Disappearance

The primary atmospheric-neutrino anomaly is the disappearance of muon neutrinos.

The observed transition is dominated by

$$\nu_\mu \rightarrow \nu_\tau \quad (163)$$

The muon-neutrino survival probability is

$$P_{\mu\mu} = 1 - P_{\mu\tau} \quad (164)$$

Experimentally, the disappearance probability is consistent with nearly maximal mixing:

$$\sin^2 (2\theta_{23}) \approx 1 \quad (165)$$

The oscillation scale is determined by

$$|\Delta m_{32}^2| \approx 2.5 \times 10^{-3} \text{ eV}^2 \quad (166)$$

This phenomenon forms one of the strongest pieces of evidence supporting neutrino oscillations.

8.4 Resonance Mixing Interpretation

Within UFQFT, atmospheric-neutrino oscillations are interpreted as resonance transformations between neutrino resonance states.

The dominant transition becomes

$$R\nu_\mu \rightarrow R\nu_\tau \quad (167)$$

The transition is driven by resonance overlap:

$$M_{\mu\tau} = \langle R\nu_\mu | R\nu_\tau \rangle \quad (168)$$

The corresponding transition probability is

$$P_{\mu\tau} = |M_{\mu\tau}|^2 \sin^2 \left(\frac{\Delta\phi_{\mu\tau}}{2} \right) \quad (169)$$

where

$$\Delta\phi_{\mu\tau} = \phi_{\mu} - \phi_{\tau} \quad (170)$$

is the resonance phase difference.

Within this framework, the observed muon-neutrino deficit arises because atmospheric neutrinos accumulate resonance phase while propagating through the Earth's fractal spacetime geometry.

8.5 Oscillation Length Analysis

The oscillation length determines the characteristic distance over which resonance conversion occurs.

The resonance oscillation length is

$$L_{osc} = \frac{2\pi\hbar c}{\Delta E_R} \quad (171)$$

where ΔE_R represents the resonance-energy difference.

Including fractal corrections yields

$$L_{osc} = \frac{2\pi\hbar c}{\Delta E_R F_D} \quad (172)$$

Atmospheric neutrinos cover distances ranging from

$$L \sim 10 \text{ km} \quad (173)$$

to

$$L \sim 1.3 \times 10^4 \text{ km} \quad (174)$$

making them highly sensitive probes of oscillation phenomena.

The observed oscillation pattern is consistent with resonance-phase accumulation over these distances.

8.6 Zenith-Angle Dependence

One of the most important signatures observed by Super-Kamiokande is the dependence of neutrino flux on zenith angle.

The zenith angle is defined as

$$\theta_z \quad (175)$$

and determines the neutrino path length through the Earth.

Downward-going neutrinos satisfy

$$\cos \theta_z \approx +1 \quad (176)$$

and travel only short distances.

Upward-going neutrinos satisfy

$$\cos \theta_z \approx -1 \quad (177)$$

and traverse nearly the entire Earth.

The survival probability therefore becomes

$$P_{\mu\mu} = P_{\mu\mu}(L(\theta_z)) \quad (178)$$

Super-Kamiokande observed a strong deficit of upward-going muon neutrinos but not downward-going neutrinos.

Within UFQFT, this behavior is naturally explained because longer propagation distances allow greater resonance-phase accumulation and therefore stronger resonance conversion.

8.7 Comparison with Experimental Data

Atmospheric-neutrino observations provide one of the most stringent tests of the resonance-mixing framework.

The relative deviation between UFQFT predictions and observations may be defined as

$$\delta_{atm} = \frac{|P_{UFQFT} - P_{exp}|}{P_{exp}} \times 100\% \quad (179)$$

The validation criterion is

$$\delta_{atm} < 5\% \quad (180)$$

for the principal atmospheric-neutrino observables.

The key datasets include:

- Super-Kamiokande,
- IceCube DeepCore,
- MINOS atmospheric measurements,
- ANTARES observations.

The resonance framework must reproduce:

- Muon-neutrino disappearance,
- Near-maximal θ_{23} mixing,
- Zenith-angle dependence,
- Energy-dependent oscillation behavior.

The correspondence principle may be expressed as

$$P_{UFQFT} \rightarrow P_{PMNS} \quad (181)$$

within the experimentally accessible regime.

The remarkable agreement between atmospheric-neutrino observations and oscillation theory therefore provides a crucial validation benchmark for UFQFT. If resonance mixing and fractal phase evolution can quantitatively reproduce these measurements, atmospheric neutrinos become strong evidence that flavor transitions may emerge from underlying resonance geometry rather than solely from conventional mass-eigenstate interference.

9. Reactor Neutrino Experiments

9.1 Reactor Antineutrino Sources

Nuclear reactors constitute some of the most intense artificial sources of electron antineutrinos. These antineutrinos are produced through the beta decay of neutron-rich fission fragments generated during nuclear fission.

The dominant fission reactions involve

$$^{235}\text{U}, ^{238}\text{U}, ^{239}\text{Pu}, ^{241}\text{Pu} \quad (182)$$

The general beta-decay process is

$$n \rightarrow p + e^- + \bar{\nu}_e \quad (183)$$

Each reactor produces an enormous antineutrino flux:

$$\Phi_R \sim 10^{20} \text{ s}^{-1} \quad (184)$$

The detection reaction commonly used in reactor experiments is inverse beta decay:

$$\bar{\nu}_e + p \rightarrow e^+ + n \quad (185)$$

Because reactors provide controlled neutrino sources with known energies and baselines, they are ideal laboratories for precision oscillation measurements.

9.2 KamLAND Results

The KamLAND experiment was designed to test neutrino oscillations using antineutrinos emitted from multiple nuclear reactors across Japan.

The average baseline was

$$L \approx 180 \text{ km} \quad (186)$$

and the characteristic neutrino energy was

$$E \sim \text{MeV} \quad (187)$$

KamLAND observed a significant deficit in the electron-antineutrino flux:

$$\frac{N_{obs}}{N_{exp}} < 1 \quad (188)$$

The measured survival probability was consistent with oscillation predictions based on solar-neutrino parameters.

The experiment provided strong confirmation of the Large Mixing Angle (LMA) solution and demonstrated that reactor antineutrinos undergo flavor transformations during propagation.

9.3 Daya Bay Measurements

The Daya Bay experiment achieved one of the most precise measurements of the mixing angle θ_{13} .

The experiment employed multiple detectors at different baselines:

$$L \sim 2 \text{ km} \quad (189)$$

The observed electron-antineutrino survival probability is

$$P_{e\bar{e}} = 1 - \sin^2(2\theta_{13}) \sin^2\left(\frac{\Delta m_{31}^2 L}{4E}\right) \quad (190)$$

The measured value was

$$\sin^2(2\theta_{13}) \approx 0.085 \quad (191)$$

This result established that θ_{13} is non-zero and opened the possibility of studying leptonic CP violation in future experiments.

Daya Bay therefore represents one of the most important precision tests of neutrino oscillation theory.

9.4 Double Chooz Results

The Double Chooz experiment independently measured reactor-antineutrino oscillations and provided additional confirmation of a non-zero θ_{13} .

The measured event ratio was

$$R = N_{obs}/N_{pred} \quad (192)$$

which showed a statistically significant deficit relative to the no-oscillation hypothesis.

The oscillation probability followed the expected baseline dependence:

$$P_{e^-e^-} = P_{e^-e^-}(L, E) \quad (193)$$

The agreement with Daya Bay strengthened confidence in the three-flavor oscillation framework and provided an important independent validation of reactor-neutrino oscillations.

9.5 RENO Experiment

The Reactor Experiment for Neutrino Oscillation (RENO) in South Korea provided another high-precision measurement of reactor-antineutrino disappearance.

The experiment used near and far detectors to reduce systematic uncertainties.

The observed survival probability was

$$P_{e^-e^-}^{RENO} < 1 \quad (194)$$

and yielded a value of θ_{13} consistent with Daya Bay and Double Chooz.

The consistency among these experiments established reactor-neutrino oscillations as one of the most precisely measured phenomena in particle physics.

The combined data significantly constrain any alternative theory of neutrino oscillations.

9.6 Resonance Interpretation of Reactor Oscillations

Within UFQFT, reactor antineutrinos are interpreted as electron-antineutrino resonance states generated through beta-decay processes.

The initial resonance state is

$$R\nu_e^- \quad (195)$$

During propagation, resonance overlap and fractal phase evolution generate transitions into other resonance configurations:

$$R\nu_e^- \rightarrow a_e R\nu_e^- + a_\mu R\nu_\mu^- + a_\tau R\nu_\tau^- \quad (196)$$

The resonance-transition probability is

$$P_{ij} = |M_{ij}|^2 \sin^2\left(\frac{\Delta\phi_{ij}}{2}\right) \quad (197)$$

where

$$M_{ij} = \langle R_i | R_j \rangle \quad (198)$$

represents the resonance-overlap matrix.

The survival probability becomes

$$P_{e\bar{e}} = 1 - P_{e\mu} - P_{e\tau} \quad (199)$$

The observed reactor-neutrino deficit is therefore interpreted as a consequence of resonance mixing rather than interference between mass eigenstates.

Because reactor experiments involve relatively short baselines and well-defined neutrino energies, they provide a particularly clean environment for testing resonance-based oscillation models.

9.7 Validation of Resonance Mixing Parameters

Reactor experiments offer some of the most precise constraints on resonance-mixing parameters.

The agreement between UFQFT predictions and experimental measurements may be quantified by

$$\delta_R = \frac{|P_{UFQFT} - P_{exp}|}{P_{exp}} \times 100\% \quad (200)$$

The validation criterion adopted in this work is

$$\delta_R < 5\% \quad (201)$$

for the principal reactor-neutrino observables.

The resonance-mixing matrix must reproduce:

- KamLAND disappearance rates,
- Daya Bay measurements of θ_{13} ,
- Double Chooz oscillation data,
- RENO survival probabilities.

The correspondence principle is

$$V_R \rightarrow U_{PMNS} \quad (202)$$

and

$$P_{UFQFT} \rightarrow P_{PMNS} \quad (203)$$

within the experimentally accessible regime.

Successful reproduction of reactor-neutrino observations would demonstrate that resonance overlap and fractal phase evolution can account for one of the most accurately measured sectors of neutrino oscillation physics. Consequently, reactor experiments represent a critical benchmark in the UFQFT Standard Model Validation Program and provide a direct test of the resonance-mixing framework developed throughout this study.

10. Long-Baseline Experiments

10.1 Principles of Long-Baseline Oscillations

Long-baseline neutrino experiments are designed to study neutrino oscillations over distances ranging from hundreds to thousands of kilometers. These experiments generate controlled neutrino beams at particle accelerators and measure the flavor composition after propagation across large distances.

The oscillation probability depends on the ratio

$$L/E \quad (204)$$

where:

- L is the baseline length,
- E is the neutrino energy.

The standard oscillation probability may be expressed as

$$P_{\alpha\beta}(L, E) \quad (205)$$

Long-baseline experiments are particularly sensitive to:

- Mixing angles,
- Mass ordering,
- Matter effects,
- CP violation.

These facilities therefore provide some of the most powerful tests of neutrino-oscillation theory.

Within UFQFT, long propagation distances allow substantial resonance-phase accumulation, making these experiments ideal probes of resonance dynamics.

10.2 T2K Experiment

The Tokai-to-Kamioka (T2K) experiment in Japan generates a muon-neutrino beam at the J-PARC accelerator facility and detects neutrinos at the Super-Kamiokande detector.

The baseline length is

$$295 \text{ km} \tag{206}$$

and the beam energy is approximately

$$E \approx 0.6 \text{ GeV} \tag{207}$$

The primary oscillation channel is

$$\nu_\mu \rightarrow \nu_e \tag{208}$$

T2K observed significant electron-neutrino appearance and provided important measurements of:

$$\theta_{13} \tag{209}$$

$$\theta_{23} \tag{210}$$

and

$$\delta_{CP} \tag{211}$$

The results indicate that neutrino oscillations occur consistently with the three-flavor framework and provide early hints of leptonic CP violation.

10.3 NOvA Experiment

The NOvA experiment in the United States studies neutrino oscillations using a beam produced at Fermilab and detected in Minnesota.

The baseline is

$$810 \text{ km} \tag{212}$$

The dominant oscillation channels are

$$\nu_\mu \rightarrow \nu_e \tag{213}$$

and

$$\nu_\mu \rightarrow \nu_\mu \tag{214}$$

NOvA provides enhanced sensitivity to:

- Neutrino mass ordering,
- CP violation,
- Matter effects.

The experiment has produced increasingly precise measurements of oscillation parameters and complements the results obtained by T2K.

Because of its longer baseline, NOvA is particularly useful for investigating propagation effects that may reveal new oscillation phenomena.

10.4 Resonance Predictions for Long Baselines

Within UFQFT, long-baseline experiments probe resonance evolution over large distances.

The resonance phase accumulated during propagation is

$$\frac{E_R L}{\hbar c} \tag{215}$$

The phase difference between resonance states becomes

$$\frac{\Delta E_R L}{\hbar c} \tag{216}$$

The transition probability is

$$|M_{ij}|^2 \sin^2\left(\frac{\Delta\phi_R}{2}\right) \tag{217}$$

Long baselines amplify resonance-phase differences and therefore enhance flavor conversion.

Including fractal corrections yields

$$\Delta\phi_0 + \delta\phi_D \tag{218}$$

where

$$\beta(D - D_c)L \tag{219}$$

This predicts that extremely long baselines may reveal small deviations from conventional oscillation models.

10.5 CP-Violation Sensitivity

One of the principal goals of long-baseline experiments is the measurement of leptonic CP violation.

In conventional oscillation theory, CP violation is characterized by the phase

$$\delta_{CP} \tag{220}$$

A difference between neutrino and antineutrino oscillation probabilities indicates CP violation:

$$P(\nu_\alpha \rightarrow \nu_\beta) \neq P(\nu_\alpha^- \rightarrow \nu_\beta^-) \quad (221)$$

Within UFQFT, CP asymmetry may emerge from resonance-phase asymmetry.

The resonance CP parameter is

$$\phi_R - \phi_R^- \quad (222)$$

The corresponding asymmetry is

$$A_{CP} = \frac{P_\nu - P_\nu^-}{P_\nu + P_\nu^-} \quad (223)$$

Future measurements of CP violation therefore provide an important opportunity to distinguish resonance-based oscillations from conventional PMNS dynamics.

10.6 Comparison with Experimental Results

Any viable oscillation model must reproduce the principal observations of T2K and NOvA.

The comparison criterion is

$$\delta = \frac{|P_{UFQFT} - P_{exp}|}{P_{exp}} \times 100\% \quad (224)$$

The validation condition adopted throughout this work is

$$\delta < 5\% \quad (225)$$

for the major oscillation observables.

The resonance framework must reproduce:

- Muon-neutrino disappearance,
- Electron-neutrino appearance,
- Energy-dependent oscillation patterns,
- Matter-induced effects,
- CP-sensitive observables.

The correspondence relation is

$$P_{UFQFT} \rightarrow P_{PMNS} \quad (226)$$

within current experimental precision.

Agreement with existing long-baseline measurements is therefore a necessary condition for validating the resonance-mixing framework.

10.7 Future Tests

The next generation of long-baseline experiments will dramatically improve sensitivity to oscillation parameters and provide unprecedented tests of UFQFT.

Important future facilities include:

- DUNE,
- Hyper-Kamiokande,
- ESSnuSB,
- P2O.

These experiments will investigate:

- Neutrino mass ordering,
- Leptonic CP violation,
- Precision oscillation parameters,
- New physics beyond the Standard Model.

Within UFQFT, future experiments may test the existence of fractal corrections through

$$P_{UFQFT} - P_{PMNS} \quad (227)$$

The relative deviation is

$$\frac{|\Delta P_D|}{P_{PMNS}} \times 100\% \quad (228)$$

A statistically significant non-zero value would indicate physics beyond the conventional PMNS framework.

Long-baseline experiments therefore represent one of the most powerful avenues for testing the resonance interpretation of neutrino oscillations. If future data reveal deviations consistent with fractal phase corrections and resonance mixing predictions, they would provide strong evidence that neutrino oscillations originate from underlying resonance geometry embedded within critical fractal spacetime rather than solely from mass-eigenstate interference.

11. Future Long-Baseline Experiments and UFQFT Predictions

11.1 DUNE Experimental Overview

The Deep Underground Neutrino Experiment (DUNE) is one of the most ambitious neutrino-physics projects currently under development. The experiment will utilize a high-intensity neutrino beam

produced at Fermilab and directed toward a large liquid-argon detector located at the Sanford Underground Research Facility.

The baseline length is

$$1300 \text{ km} \quad (229)$$

making DUNE one of the longest-baseline neutrino experiments ever constructed.

The primary scientific objectives include:

- Determination of neutrino mass ordering,
- Measurement of leptonic CP violation,
- Precision oscillation studies,
- Searches for physics beyond the Standard Model.

The large baseline enhances matter effects and increases sensitivity to subtle deviations from conventional oscillation theory.

Within UFQFT, DUNE provides an ideal environment for testing resonance-phase evolution over very large propagation distances.

11.2 Hyper-Kamiokande Overview

Hyper-Kamiokande represents the next-generation successor to Super-Kamiokande and will be the largest water Cherenkov detector ever constructed.

The experiment will receive neutrino beams from J-PARC and operate with a baseline of

$$295 \text{ km} \quad (230)$$

while simultaneously observing atmospheric, solar, and astrophysical neutrinos.

Its primary objectives include:

- Precision measurements of oscillation parameters,
- CP-violation searches,
- Atmospheric-neutrino studies,
- Proton-decay searches.

The enormous detector volume will provide unprecedented statistical precision.

Consequently, Hyper-Kamiokande is expected to become one of the most important experimental tests of neutrino oscillation physics during the coming decades.

11.3 Resonance-Based Oscillation Predictions

Within UFQFT, neutrino oscillations arise from resonance mixing and fractal phase evolution.

The resonance-transition probability is

$$|M_{ij}|^2 \sin^2\left(\frac{\Delta\phi_R}{2}\right) \quad (231)$$

where

$$\langle R_i | R_j \rangle \quad (232)$$

is the resonance-overlap matrix.

The accumulated resonance phase is

$$\frac{E_R L}{\hbar c} \quad (233)$$

For extremely long baselines such as DUNE,

$$L \gg L_{osc} \quad (234)$$

small geometric corrections may become experimentally observable.

UFQFT therefore predicts that future high-precision oscillation measurements could reveal subtle deviations from the standard PMNS framework.

11.4 Fractal Corrections to Oscillation Patterns

A distinctive prediction of UFQFT is the existence of fractal corrections arising from the geometric structure of spacetime.

The total resonance phase may be expressed as

$$\phi_0 + \delta\phi_D \quad (235)$$

where

$$\beta(D-D_c)L \quad (236)$$

and

$$D_c \approx 2.7 \quad (237)$$

is the critical fractal dimension.

The oscillation probability becomes

$$P_{PMNS} + \Delta P_D \quad (238)$$

where

$$f(D,E,L) \tag{239}$$

represents the fractal correction.

The correction is expected to be small but may become detectable through precision measurements at future facilities.

11.5 Expected Signatures Beyond the Standard Model

If UFQFT correctly describes neutrino oscillations, several observable signatures may emerge beyond conventional PMNS predictions.

Possible signatures include:

- Small energy-dependent deviations in oscillation probabilities,
- Baseline-dependent resonance corrections,
- Modified matter effects,
- Additional phase shifts in appearance channels,
- Enhanced sensitivity to spacetime geometry.

The deviation from conventional theory may be written as

$$P_{UFQFT} - P_{PMNS} \tag{240}$$

The corresponding relative difference is

$$\frac{|\Delta P|}{P_{PMNS}} \times 100\% \tag{241}$$

Detection of statistically significant deviations would provide evidence for new oscillation physics beyond the Standard Model.

11.6 Distinguishing UFQFT from PMNS Predictions

A central objective of future experiments is determining whether resonance-based oscillations can be experimentally distinguished from conventional PMNS oscillations.

The Standard Model prediction is

$$P_{PMNS} \tag{242}$$

while UFQFT predicts

$$P_{PMNS} + \Delta P_D \tag{243}$$

The distinguishing observable becomes

$$P_{UFQFT} - P_{SM} \quad (244)$$

Several measurements may be particularly sensitive:

- Electron-neutrino appearance rates,
- Muon-neutrino disappearance rates,
- CP-asymmetry measurements,
- Energy-spectrum distortions,
- Baseline-dependent phase effects.

The longer baseline of DUNE makes it especially sensitive to accumulated resonance-phase corrections, while Hyper-Kamiokande offers exceptional statistical precision for detecting subtle oscillation anomalies.

11.7 Experimental Validation Strategy

The validation strategy for UFQFT consists of systematic comparison between theoretical predictions and future experimental data.

The agreement criterion is defined as

$$\delta_{exp} = \frac{|P_{UFQFT} - P_{obs}|}{P_{obs}} \times 100\% \quad (245)$$

The primary validation condition is

$$\delta_{exp} < 5\% \quad (246)$$

for the principal oscillation observables.

The validation program should include:

- Solar-neutrino datasets,
- Atmospheric-neutrino datasets,
- Reactor-neutrino measurements,
- T2K and NOvA results,
- DUNE observations,
- Hyper-Kamiokande observations.

The correspondence principle remains

$$P_{UFQFT} \rightarrow P_{PMNS} \quad (247)$$

within current experimental uncertainties.

However, if future experiments identify statistically significant deviations satisfying

$$\Delta P_D \neq 0 \quad (248)$$

the resonance framework would gain strong experimental support.

DUNE and Hyper-Kamiokande therefore represent the most important future tests of neutrino oscillations within UFQFT. Their combination of long baselines, high statistics, and precision measurements provides an unprecedented opportunity to investigate whether resonance mixing and fractal spacetime corrections constitute a deeper physical origin of neutrino flavor transformation beyond the conventional PMNS paradigm.

12. Standard Model versus UFQFT

12.1 Nature of Neutrinos

The Standard Model originally described neutrinos as massless fundamental leptons participating only in weak and gravitational interactions. Following the discovery of neutrino oscillations, the framework was extended to accommodate non-zero neutrino masses, although the fundamental origin of these masses remains unresolved.

The three known neutrino flavors are

$$\nu_e, \nu_\mu, \nu_\tau \quad (249)$$

and are treated as elementary particles.

In contrast, UFQFT interprets neutrinos as stable resonance configurations arising from coupled Φ and Ψ fields.

The general neutrino resonance state is

$$R(n, D, \theta) \quad (250)$$

where:

- n denotes resonance level,
- D denotes fractal dimension,
- θ denotes resonance phase.

Within this framework, neutrinos are not fundamental objects but emergent resonance structures embedded in fractal spacetime.

12.2 Origin of Oscillations

In the Standard Model extension, neutrino oscillations arise because flavor eigenstates differ from mass eigenstates.

The flavor state is written as

$$\sum_i U_{\alpha i} | \nu_i \rangle \quad (251)$$

and phase differences accumulate during propagation.

Consequently, oscillations emerge from interference between mass eigenstates.

Within UFQFT, oscillations originate from resonance evolution.

The resonance transition is

$$R_i \rightarrow R_j \quad (252)$$

and is driven by resonance overlap and phase evolution.

The accumulated resonance phase is

$$\frac{E_R L}{\hbar c} \quad (253)$$

Thus, flavor transformation emerges from geometric resonance dynamics rather than mass-state interference alone.

12.3 Flavor Mixing

The Standard Model describes flavor mixing through the PMNS matrix.

The transformation is

$$\sum_i U_{ai} | \nu_i \rangle \quad (254)$$

where the matrix elements are experimentally determined.

The values of the mixing parameters are not predicted by the theory and must be measured experimentally.

UFQFT instead attributes flavor mixing to resonance overlap.

The overlap matrix is

$$\langle R_i | R_j \rangle \quad (255)$$

The transition probability becomes

$$| M_{ij} |^2 \quad (256)$$

Therefore, flavor mixing is interpreted as a geometric property of resonance space rather than a fundamental input parameter.

12.4 PMNS Matrix versus Resonance Mixing Matrix

The PMNS matrix plays a central role in conventional neutrino oscillation theory.

It may be written as

$$\begin{pmatrix} U_{e1} & U_{e2} & U_{e3} \\ U_{\mu1} & U_{\mu2} & U_{\mu3} \\ U_{\tau1} & U_{\tau2} & U_{\tau3} \end{pmatrix} \quad (257)$$

Within UFQFT, the analogous quantity is the resonance mixing matrix:

$$\begin{pmatrix} M_{ee} & M_{e\mu} & M_{e\tau} \\ M_{\mu e} & M_{\mu\mu} & M_{\mu\tau} \\ M_{\tau e} & M_{\tau\mu} & M_{\tau\tau} \end{pmatrix} \quad (258)$$

The correspondence principle is

$$V_R \rightarrow U_{PMNS} \quad (259)$$

in the experimentally accessible limit.

The crucial distinction is that PMNS elements are empirical parameters, whereas resonance-matrix elements are intended to emerge from resonance geometry.

12.5 Oscillation Mechanism

The standard oscillation probability for two flavors is

$$\sin^2(2\theta) \sin^2\left(\frac{\Delta m^2 L}{4E}\right) \quad (260)$$

which depends on mass-squared differences and mixing angles.

In UFQFT, the corresponding probability is

$$|M_{ij}|^2 \sin^2\left(\frac{\Delta\phi_R}{2}\right) \quad (261)$$

where

$$\phi_i - \phi_j \quad (262)$$

The mathematical forms are similar, but the physical interpretation differs fundamentally.

The Standard Model relies on quantum interference between mass eigenstates, whereas UFQFT attributes oscillations to resonance-phase evolution and geometric overlap.

12.6 Role of Spacetime Geometry

In conventional oscillation theory, spacetime serves primarily as a propagation background.

Oscillation dynamics depend mainly on

$$L \quad (263)$$

and

$$E \quad (264)$$

with geometry playing only an indirect role through matter effects.

UFQFT assigns a central role to spacetime geometry.

The local fractal dimension is

$$D(x^\mu) \quad (265)$$

and oscillation dynamics explicitly depend on

$$D_c \approx 2.7 \quad (266)$$

The fractal phase correction is

$$\beta(D - D_c)L \quad (267)$$

This introduces a direct connection between neutrino oscillations and the geometric structure of spacetime.

Consequently, oscillation experiments become potential probes of fractal geometry.

12.7 Comparative Summary Table

Feature	Standard Model	UFQFT
Nature of Neutrinos	Fundamental particles	Resonance states
Neutrino Ontology	Elementary leptons	Φ - Ψ resonances
Origin of Mass	Beyond original SM	Resonance localization
Oscillation Source	Mass-state interference	Resonance evolution
Flavor Mixing	PMNS matrix	Resonance overlap
Mixing Parameters	Experimental inputs	Geometric quantities

Feature	Standard Model	UFQFT
Propagation States	Mass eigenstates	Resonance eigenstates
Oscillation Driver	Phase difference from masses	Resonance phase accumulation
Role of Geometry	Secondary	Fundamental
Spacetime Structure	Continuous manifold	Fractal spacetime
Critical Parameter	Δm^2	$D \approx 2.7$
Matter Effects	MSW mechanism	Fractal resonance modification
Experimental Description	Established	Under development
Mathematical Basis	Quantum field theory	Resonance geometry
Ultimate Goal	Describe oscillations	Explain origin of oscillations

12.8 Summary

The comparison demonstrates that UFQFT does not seek to replace the successful phenomenology of neutrino oscillation experiments. Rather, it proposes a deeper physical interpretation in which flavor transformations emerge from resonance geometry and fractal spacetime dynamics.

While the Standard Model provides an exceptionally accurate description of *how* oscillations occur, UFQFT attempts to explain *why* flavor mixing exists and how it may arise from a more fundamental resonance-based structure of nature.

Future experimental tests involving DUNE, Hyper-Kamiokande, and next-generation neutrino facilities will determine whether resonance-based corrections can be distinguished from conventional PMNS predictions and whether neutrino oscillations provide evidence for a deeper fractal organization of spacetime.

13. Discussion

13.1 Neutrino Oscillations as Resonance Transformations

The central proposition of this study is that neutrino oscillations may be interpreted as resonance transformations occurring within the framework of Unified Fractal Quantum Field Theory. In the conventional PMNS formalism, flavor transitions arise because neutrino flavor eigenstates are quantum

superpositions of mass eigenstates that accumulate different phases during propagation. While this approach successfully reproduces experimental observations, it does not provide a fundamental explanation for the origin of flavor mixing itself.

UFQFT proposes an alternative interpretation in which neutrinos are viewed as resonance structures emerging from coupled Φ and Ψ fields embedded within fractal spacetime. Oscillations are therefore not transitions between fundamental mass states but geometric transformations among resonance configurations. The observed flavor evolution emerges naturally from resonance overlap, phase accumulation, and fractal spacetime dynamics.

From this perspective, neutrino oscillations represent a manifestation of deeper geometric processes occurring within the underlying resonance structure of matter.

13.2 Emergent Flavor Symmetry

A notable consequence of the resonance framework is the possibility that flavor symmetry is not fundamental but emergent.

In the Standard Model, flavor states are introduced as independent degrees of freedom, and the PMNS matrix is required to connect flavor and mass eigenstates. The physical origin of the observed mixing pattern remains unknown.

Within UFQFT, flavor states correspond to different resonance levels belonging to a common resonance hierarchy. The observed mixing arises because these resonance states possess finite geometric overlap and evolve dynamically during propagation.

Consequently, flavor symmetry may emerge as a macroscopic manifestation of resonance geometry rather than as a fundamental property of elementary particles. If correct, this interpretation could provide a unified explanation for the existence of flavor mixing across both neutrino and quark sectors.

13.3 Advantages of the Resonance Framework

The resonance interpretation offers several conceptual advantages.

First, it provides a common physical mechanism connecting neutrino oscillations, particle masses, weak interactions, and resonance dynamics. Rather than introducing separate structures for each phenomenon, UFQFT attempts to derive them from a single geometric framework.

Second, the theory naturally incorporates spacetime geometry into oscillation physics. Conventional oscillation models treat spacetime primarily as a passive background, whereas UFQFT predicts that geometric properties directly influence oscillation behavior through fractal phase evolution.

Third, the resonance framework offers a possible explanation for the origin of flavor mixing. Instead of treating mixing parameters as purely empirical quantities, it seeks to derive them from resonance overlap and geometric structure.

Finally, the model generates experimentally testable predictions involving fractal corrections, resonance-induced phase shifts, and potential deviations from standard oscillation patterns.

13.4 Current Limitations

Despite its conceptual appeal, the present UFQFT formulation remains incomplete and faces several important challenges.

The most significant limitation is the absence of a fully derived resonance-mixing matrix capable of predicting all experimentally measured oscillation parameters from first principles. At present, the correspondence between resonance mixing and the PMNS framework remains largely phenomenological.

A second limitation concerns the quantitative determination of resonance coupling strengths and fractal correction coefficients. These parameters require further theoretical development before precise predictions can be generated.

Additionally, the mathematical foundations of fractal spacetime remain under active investigation. Important questions concerning covariance, quantization, renormalization, and the microscopic origin of the critical dimension ($D=2.7$) have not yet been completely resolved.

Consequently, UFQFT should currently be regarded as an exploratory theoretical framework rather than a fully established alternative to the Standard Model.

13.5 Implications for Particle Physics

If the resonance interpretation proves correct, the implications for particle physics would be substantial.

The conventional distinction between particles and interactions would be replaced by a unified description based on resonance structures. Neutrino oscillations, weak interactions, mass generation, and flavor transitions could then be interpreted as different manifestations of the same underlying resonance dynamics.

Such a framework might also provide insight into several unresolved questions:

- Origin of neutrino masses,
- Origin of flavor mixing,
- Mass hierarchy problem,
- Relationship between quarks and leptons,
- Nature of electroweak interactions.

The resonance perspective therefore suggests a possible route toward a deeper understanding of particle physics beyond the Standard Model.

13.6 Implications for Cosmology

Neutrinos play a central role in cosmology, influencing structure formation, cosmic evolution, and the thermal history of the Universe.

Within UFQFT, neutrino oscillations become directly linked to spacetime geometry through fractal phase evolution. This connection introduces the possibility that cosmological evolution and particle dynamics are governed by common geometric principles.

Potential cosmological implications include:

- Modified neutrino propagation over cosmological distances,
- Geometric contributions to dark-sector phenomena,
- Resonance-based interpretations of cosmic neutrino backgrounds,
- Connections between neutrino physics and fractal spacetime evolution.

If confirmed, these effects could establish a direct relationship between particle physics and large-scale cosmic structure.

13.7 Future Directions

Several research directions emerge from the present work.

The first priority is the development of a fully predictive resonance-mixing theory capable of deriving oscillation parameters directly from resonance geometry. Such a framework would significantly strengthen the quantitative foundations of UFQFT.

A second objective is the extension of the model to leptonic CP violation. Future studies should investigate whether resonance-phase asymmetries can reproduce the CP-violating effects currently being explored by T2K, NOvA, DUNE, and Hyper-Kamiokande.

Additional research should examine:

- Matter–antimatter asymmetry,
- Sterile-neutrino scenarios,
- Cosmological neutrino propagation,
- High-energy astrophysical neutrinos,
- Unified quark–lepton resonance structures.

Finally, future experimental data from DUNE and Hyper-Kamiokande will provide the most stringent tests of the resonance framework. The detection of statistically significant deviations from PMNS predictions would offer important evidence supporting resonance-based oscillation dynamics and the broader UFQFT program.

Taken together, the results of this study suggest that neutrino oscillations may provide one of the most accessible experimental windows into the deeper resonance structure proposed by Unified Fractal Quantum Field Theory. While substantial theoretical work remains necessary, the resonance interpretation offers a coherent and potentially testable framework linking neutrino physics, spacetime geometry, and the fundamental organization of matter.

14. Conclusions

Neutrino oscillations constitute one of the most important discoveries in modern particle physics, providing direct evidence that neutrinos possess non-zero masses and that the Standard Model is incomplete in its original formulation. The conventional description based on the PMNS mixing matrix has achieved remarkable success in explaining solar, atmospheric, reactor, and accelerator neutrino experiments. Nevertheless, fundamental questions concerning the origin of neutrino masses, flavor mixing, and oscillation dynamics remain unresolved. The Standard Model effectively describes how neutrino oscillations occur but does not fully explain why flavor transformations exist at a deeper physical level.

In this work, a comprehensive interpretation of neutrino oscillations has been developed within the framework of Unified Fractal Quantum Field Theory (UFQFT). The theory proposes that neutrinos are not fundamental particles but stable resonance configurations emerging from coupled energy (Φ) and charge (Ψ) fields embedded in a fractal spacetime characterized by a critical dimension near ($D = 2.7$). Within this framework, flavor transitions are interpreted as resonance transformations driven by geometric overlap, resonance mixing, and fractal phase evolution rather than by interference among fundamental mass eigenstates.

A resonance-mixing formalism was introduced to describe electron-, muon-, and tau-neutrino transformations. The resulting framework reproduces the qualitative structure of the PMNS description while providing an alternative physical interpretation based on resonance geometry. Oscillation probabilities were derived from resonance overlap matrices and phase accumulation in fractal spacetime, establishing a direct connection between neutrino behavior and the geometric properties of the underlying spacetime structure.

The resonance framework was subsequently applied to the principal experimental domains of neutrino physics. Solar-neutrino observations, atmospheric-neutrino measurements, reactor-antineutrino experiments, and long-baseline accelerator studies were examined as validation benchmarks. In each case, the theory demonstrated how the observed flavor transitions may be interpreted as manifestations of resonance dynamics. Particular emphasis was placed on future experimental programs such as DUNE and Hyper-Kamiokande, which offer unprecedented opportunities to test resonance-based predictions and search for deviations from conventional PMNS behavior.

A central result of this study is the proposal that flavor mixing may be an emergent phenomenon arising from resonance geometry rather than a fundamental property introduced through independent mixing parameters. In this interpretation, the PMNS matrix represents an effective low-energy manifestation of a deeper resonance-mixing structure. This perspective provides a possible route toward understanding the physical origin of flavor transitions and may ultimately contribute to a more unified description of particle masses, weak interactions, and neutrino dynamics.

At the same time, important challenges remain. The present formulation has not yet derived all oscillation parameters directly from first principles, and several aspects of the resonance-mixing framework require further theoretical development. In particular, the quantitative determination of resonance coupling strengths, fractal correction coefficients, and CP-violating effects remains an important objective for future work. Consequently, UFQFT should currently be regarded as a developing theoretical framework whose validity must be assessed through rigorous comparison with experimental observations.

Future investigations will focus on leptonic CP violation, matter–antimatter asymmetry, sterile-neutrino scenarios, and cosmological neutrino propagation. The next generation of neutrino experiments will play a decisive role in determining whether resonance-based oscillation dynamics can be experimentally distinguished from conventional PMNS predictions. Any statistically significant and reproducible deviation consistent with resonance-phase corrections would provide strong support for the UFQFT interpretation.

In conclusion, this study demonstrates that neutrino oscillations can be consistently interpreted within the resonance-based framework of Unified Fractal Quantum Field Theory. By connecting flavor transformations to resonance geometry and fractal spacetime dynamics, UFQFT offers a novel perspective on one of the most important phenomena in modern physics. Whether this framework represents a deeper physical description of neutrino behavior remains an open question, but the theory generates clear experimental targets and establishes a foundation for future investigations. As a result, neutrino oscillations emerge as a promising testing ground for exploring the broader resonance-geometric structure proposed by UFQFT and for probing the possible fractal nature of spacetime itself.

References

- Abe, K., et al. (2018). *Hyper-Kamiokande Design Report*. arXiv:1805.04163.
- Abe, K., et al. (2020). Constraint on the matter–antimatter symmetry-violating phase in neutrino oscillations. *Nature*, 580(7803), 339–344.
- Abi, B., et al. (2020). Deep Underground Neutrino Experiment (DUNE), Far Detector Technical Design Report. *Journal of Instrumentation*, 15, T08008.
- Acero, M. A., et al. (2022). An improved measurement of neutrino oscillation parameters by the NOvA experiment. *Physical Review D*, 106(3), 032004.
- Ahmad, Q. R., et al. (2002). Direct evidence for neutrino flavor transformation from neutral-current interactions in the Sudbury Neutrino Observatory. *Physical Review Letters*, 89(1), 011301.
- Ahn, J. K., et al. (2012). Observation of reactor electron antineutrino disappearance in the RENO experiment. *Physical Review Letters*, 108(19), 191802.
- ALEPH Collaboration, DELPHI Collaboration, L3 Collaboration, OPAL Collaboration, & SLD Collaboration. (2006). Precision electroweak measurements on the Z resonance. *Physics Reports*, 427(5–6), 257–454.
- An, F. P., et al. (2012). Observation of electron-antineutrino disappearance at Daya Bay. *Physical Review Letters*, 108(17), 171803.
- Bahcall, J. N. (1964). Solar neutrinos I. Theoretical. *Physical Review Letters*, 12(11), 300–302.
- Davis, R., Harmer, D. S., & Hoffman, K. C. (1968). Search for neutrinos from the Sun. *Physical Review Letters*, 20(21), 1205–1209.

Eguchi, K., et al. (2003). First results from KamLAND: Evidence for reactor antineutrino disappearance. *Physical Review Letters*, 90(2), 021802.

Fermi, E. (1934). Versuch einer Theorie der β -Strahlen. *Zeitschrift für Physik*, 88(3–4), 161–177.

Fukuda, Y., et al. (1998). Evidence for oscillation of atmospheric neutrinos. *Physical Review Letters*, 81(8), 1562–1567.

Fukuda, Y., et al. (2001). Solar 8B and hep neutrino measurements from 1258 days of Super-Kamiokande data. *Physical Review Letters*, 86(25), 5651–5655.

Gonzalez-Garcia, M. C., & Maltoni, M. (2008). Phenomenology with atmospheric neutrinos. *Physics Reports*, 460(1–3), 1–129.

Maki, Z., Nakagawa, M., & Sakata, S. (1962). Remarks on the unified model of elementary particles. *Progress of Theoretical Physics*, 28(5), 870–880.

Mikheyev, S. P., & Smirnov, A. Y. (1985). Resonance enhancement of oscillations in matter and solar neutrino spectroscopy. *Soviet Journal of Nuclear Physics*, 42, 913–917.

Minkowski, P. (1977). $\mu \rightarrow e\gamma$ at a rate of one out of 10^9 muon decays? *Physics Letters B*, 67(4), 421–428.

Mohapatra, R. N., & Senjanović, G. (1980). Neutrino mass and spontaneous parity nonconservation. *Physical Review Letters*, 44(14), 912–915.

Particle Data Group. (2024). *Review of Particle Physics*. *Progress of Theoretical and Experimental Physics*, 2024, 083C01.

Pauli, W. (1930). Letter to the Physical Society of Tübingen.

Pontecorvo, B. (1957). Mesonium and antimesonium. *Soviet Physics JETP*, 6, 429–431.

Reines, F., & Cowan, C. L. (1956). Detection of the free neutrino. *Physical Review*, 92(3), 830–831.

^aSogukpinar, H. Unified Fractal Quantum Field Theory (UFQFT): Matter as Geometric Resonances of Unified Energy-Charge Fields. Preprint, ScienceOpen . 2025.

^bSogukpinar, H. The Φ_0 - Ψ_0 Fractal Sea of Pre-Big Bang Universe: A Unified Origin of Matter, Dark Matter, and Cosmic Inflation from UFQFT. Preprint, ScienceOpen . 2025.

^cSogukpinar, H. Proton Spin Structure Reinterpreted through UFQFT. Preprint, ScienceOpen . 2025.

^dSogukpinar, H. Dark Matter and Dark Energy in Unified Fractal Quantum Field Theory (UFQFT): Neutral Resonances and Non-Material Oscillations. Preprint, ScienceOpen . 2025.

^eSogukpinar, H. What Is Time: Deriving the Arrow of Fractal Spacetime Framework from UFQFT. Preprint, ScienceOpen . 2025.

^fSogukpinar, H. Gravity and Gravitation in UFQFT: An Emergent Phenomenon from Fractal Field Symmetry. Preprint, ScienceOpen . 2025.

^gSogukpinar, H. From Quarks to Neutrinos: A Fractal Framework for Elementary Particle Hierarchy. Preprint, ScienceOpen . 2025.

^hSogukpinar, H. HALO Nuclei Beyond the Shell Model: A Fractal-Dimensional Approach. Preprint, ScienceOpen , 2025.

ⁱSogukpinar, H. Fractal Geometry in Atomic Nuclei: A New Paradigm for Nuclear Structure and Decay. Preprint, ScienceOpen . 2025.

^kSogukpinar, H. The Bubble-UFQFT Framework: Unifying Quantum Gravity, Dark Energy, and Cosmological Structure. Preprint, ScienceOpen . 2025.

^lSogukpinar, H. The Bubble Theory of the Universe: A Quantum Fluid Perspective on Cosmological Emergence. Preprint, ScienceOpen . 2025.

^mSogukpinar, H. Neutron Stars as Fractal Dipole Liquids: A Unified Fractal Quantum Field Theory Approach. Preprint, ScienceOpen . 2025.

ⁿSogukpinar, H. The Critical Mass-Limit in Black Hole Evolution: A Prediction of Unified Fractal Quantum Field. Preprint, ScienceOpen . 2025.

^oSogukpinar, H. Proton and Neutron Properties from Unified Fractal Quantum Field Theory (UFQFT): A Resonance-Based Approach to Mass, Spin, and Binding Energies. Preprint, ScienceOpen . 2025.

^pSogukpinar, H. Charged and Neutral Particle Collisions in High-Energy Accelerators: A Unified Fractal Quantum Field Theory Perspective (UFQFT). Preprint, ScienceOpen . 2025..

^rSogukpinar, H. Fractal Resonance and the Emergence of Charge: Energy–Charge Duality in UFQFT. Preprint, ScienceOpen . 2025.

^sSogukpinar, H. CP Violation in Unified Fractal Quantum Field Theory: Resonance Asymmetry and Connections to Dark Sector Physics. ScienceOpen . 2025.

^tSogukpinar, H. Matter–Antimatter Resonances in Unified Fractal Quantum Field Theory (UFQFT): Fractal Phase Inversions, Stability Asymmetries, and the Origin of Baryogenesis. ScienceOpen . 2025.

^uSogukpinar, H. Mesons as Fractal Resonance States: A Unified Fractal Quantum Field Theory (UFQFT) Perspective. ScienceOpen . 2025.

^vSogukpinar, H. Weak Interactions as Φ – Ψ Resonances: A Unified Fractal Quantum Field Theory (UFQFT) Approach Beyond the W/Z Bosons. Preprint, ScienceOpen . 2025.

^wSogukpinar, H. Origin of Mass in UFQFT: From the Higgs Mechanism to Fractal Resonance in Unified Fractal Quantum Field Theory .Preprint, ScienceOpen . 2025.

^zSogukpinar, H. Lagrangian and Hamiltonian Formalism in Unified Fractal Quantum Field Theory (UFQFT).Preprint, ScienceOpen . 2025.

^{1a}Sogukpinar, H. Neutrino Oscillations as Φ – Ψ Phase Resonance Transitions in Unified Fractal Quantum Field Theory (UFQFT).Preprint, ScienceOpen . 2025.

^{1b}Sogukpinar, H. Resolving Standard Model Anomalies through Unified Fractal Quantum Field Theory (UFQF).Preprint, ScienceOpen . 2025.

^{1c}Sogukpinar, H. Electromagnetic Waves as Φ – Ψ Resonance Modes in Fractal Spacetime: Unified Fractal Quantum Field Theory (UFQFT) Approach. Preprint, ScienceOpen . 2025.

^{1d}Sogukpinar, H. Fractal Cosmology and Particle Stability: A Unified Field Perspective in UFQFT. Preprint, ScienceOpen . 2025.

^{1e}Sogukpinar, H. Fractal Quantum Architecture of Matter: A Unified Framework for Particle Physics. Preprint, ScienceOpen . 2025.

^{1d}Sogukpinar, General Relativity as the Classical Limit of the Unified Fractal Quantum Field Theory (UFQFT). Preprint, ScienceOpen . 2025.

^{1f}Sogukpinar, Time Dilation, Length Contraction, And Spacetime Curvature of Relativistic Phenomena in the Unified Fractal Quantum Field Theory (UFQFT). Preprint, ScienceOpen . 2025.

^{1g}Sogukpinar, Advancing the Unified Fractal Quantum Field Theory: Quantization, Microscopic Potentials, and Standard Model Precision Tests, Preprint, ScienceOpen . 2025.

^{1h}Sogukpinar, Experimental Signatures of Unified Fractal Quantum Field Theory (UFQFT): From Particle Resonances to Cosmological Observations, Preprint, ScienceOpen . 2025.

¹ⁱSogukpinar, Unified Fractal Quantum Field Theory (UFQFT) A Geometric Unification of Matter, Dark Matter, and Dark Energy Through Energy-Charge Field Dynamics. 2025.

^{1k}Sogukpinar, Resonance-Selective Baryogenesis in the Early Universe: A Unified Fractal Quantum Field Theory (UFQFT) Explanation for Matter-Dominated Evolution, Preprint, ScienceOpen . 2025.

^{1l}Sogukpinar, Fractal Spacetime and Unified Φ - Ψ Fields: A Comprehensive Framework for Matter, Forces, and the Universe in the Unified Fractal Quantum Field Theory (UFQFT), Preprint, ScienceOpen . 2025.

Wolfenstein, L. (1978). Neutrino oscillations in matter. *Physical Review D*, 17(9), 2369–2374.